Available online at www.sciencedirect.com
ScienceDirect
European Journal of Pharmaceutics and Biopharmaceutics 70 (2008) 153–164
European Journal of Pharmaceutics and Biopharmaceutics
www.elsevier.com/locate/ejpb

Research paper

# Liposomal vasoactive intestinal peptide for lung application: Protection from proteolytic degradation

Brigitte Stark [a], Fritz Andreae [b], Wilhelm Mosgoeller [c], Michael Edetsberger [d], Erwin Gaubitzer [d], Gottfried Koehler [d], Ruth Prassl [a,*]

[a] *Institute of Biophysics and Nanosystems Research, Austrian Academy of Sciences, Graz, Austria*
[b] *piCHEM Research & Development, Graz, Austria*
[c] *Institute of Cancer Research, Medical University of Vienna, Vienna, Austria*
[d] *Max F. Perutz Laboratories, University of Vienna, Vienna, Austria*

Received 17 October 2007; accepted in revised form 17 April 2008
Available online 27 April 2008

**Abstract**

Inhalative administration of vasoactive intestinal peptide (VIP) is a promising approach for the treatment of severe lung diseases. However, the clinical use of VIP is limited by the fact that the peptide is prone to rapid degradation mechanisms and proteolytic digestion. Accordingly, VIP exhibits a very short period of activity in the lung. To overcome this problem, we have designed a liposomal drug delivery system for VIP and characterized it in terms of its potential to protect VIP from enzymatic cleavage. The proteolytic conditions of the lung, the target site of aerosolic administered VIP, were mimicked by bronchoalveolar lavage fluid (BALF), a lung surfactant solution, obtained by fiberoptic bronchoscopy. Thus, the stability of VIP was assessed by its resistance to enzymatic degradation in BALF, using a combination of high pressure liquid chromatography with mass spectrometry. We found that free VIP was rapidly digested, whereas liposomal-associated VIP remained intact. By fluorescence spectroscopic techniques using fluorescent-labelled VIP we got strong indications that the tight association of VIP with the lipid membrane is only minimally affected upon incubation with BALF. Loading capacity and stability of EtCy3-VIP loaded liposomes were measured by fluorescence fluctuation spectroscopy. Finally, the protective properties of the liposomes were also expressed in the maintained biological activity of the peptide incubated with BALF.


*Keywords:* Liposomes; VIP; Pulmonary delivery; Proteolytic degradation

## 1. Introduction

Vasoactive intestinal peptide (VIP) is a cationic 28 amino acid peptide and a member of the secretin/glucagon family [1]. It is widely distributed within the body, including lung, gastrointestinal tract, heart, kidney and brain [2]. VIP exerts a variety of biological functions, including pulmonary and bronchodilation [3], vasodilation [4], smooth muscle relaxation [1], anti-inflammatory and immunomodulatory effects [4–6]. Moreover, it functions as a neurotransmitter and neuromodulator [7]. VIP performs its biological effects through specific, G-protein-coupled membrane receptors, namely $VPAC_1$, $VPAC_2$ and $PAC_1$ [8,9].

*Abbreviations:* VIP, vasoactive intestinal peptide; POPC, palmitoyl-oleoyl-phosphatidylcholine; lyso-PG, lyso-stearyl-phosphatidyl-glycerol; DSPE-PEG2000, polyethyleneglycol ($M_W = 2000$) covalently linked to distearyl-phosphatidylethanolamine; KH-buffer, Krebs–Henseleit-buffer; TFA, trifluoroacetic acid; NEP, neutral endopeptidase; ELF, epithelial lining fluid; BAL, bronchoalveolar lavage; BALF, bronchoalveolar lavage fluid; PCS, photon correlation spectroscopy; PDI, polydispersity index; FFS, fluorescence fluctuation spectroscopy; FCS, fluorescence correlation spectroscopy; PCH, photon counting histogramming; FIDA, fluorescence intensity distribution analysis; HPLC, high performance liquid chromatography; MS, mass spectrometry; MALDI-TOF, matrix assisted laser desorption/ionization-time of flight; VLL, VIP loaded liposomes; Trp-VIP, Trp residue attached to the N-terminus of VIP; EtCy3-VIP, fluorescent marker Cy3 coupled to the N-terminal amino group of His.

* Corresponding author. Institute of Biophysics and Nanosystems Research, Austrian Academy of Sciences, Schmiedlstr.6, A-8042 Graz, Austria. Tel.: +43 316 4120 305.
*E-mail address:* ruth.prassl@oeaw.ac.at (R. Prassl).

0939-6411/$ - see front matter © 2008 Elsevier B.V. All rights reserved.
doi:10.1016/j.ejpb.2008.04.015

As several diseases are characterized by a deficiency of VIP in the tissue, a treatment with exogenous VIP was suggested to result in a therapeutic benefit [5]. Among these disorders are cystic fibrosis [10], ulcerative colitis [11] and primary pulmonary hypertension (PPH) [2,6]. The latter is a lung disease of unknown origin, which is characterized by persistent elevation of the pulmonary artery pressure [12]. According to this, the small blood vessels in the lung undergo changes, resulting in resistance to blood flow through the lung circulation [13]. Petkov et al. [6] demonstrated that PPH patients display, beside a lack of VIP, an increased VIP-receptor expression and binding affinity. Moreover, this group showed the suitability of pulmonary application of exogenous VIP for the treatment of PPH although the half-life time of VIP in the lung was extremely short.

In other lung diseases, such as asthma or chronic obstructive pulmonary diseases, however, the expression of VIP-degrading proteases is significantly increased [14,15], a fact, which again hampers the clinical use of VIP as a therapeutic agent.

Generally, the pulmonary administration route of drugs, which act in the respiratory tract, exhibits several advantages over alternative routes, including a rapid drug effect at the site of action, a reduced dose, a reduction in systemic side-effects, the evasion of first pass hepatic metabolism [16] and an enhanced bioavailability of the delivered drug [17].

However, the biological effects of inhaled VIP are short-lived, due to several degradation mechanisms including spontaneous hydrolysis [2], enzymatic cleavage by, for instance, neutral endopeptidases (NEP) [4,18], mast cell chymase and mast cell tryptase [19], or antibody-catalyzed degradation [7]. The most prevalent cleaving sites of VIP by NEP are at the amino acid positions 7–8 (Thr-Asp) and 25–26 (Ser-Ile), which leads to the major cleavage products, VIP1–25 and VIP26–28 and to a less extent to VIP1–7 and VIP 8–28 [4]. To this end, all these fragments are no longer physiologically active [20].

Accordingly, to circumvent these degradation problems, stable analogues of VIP were synthesized by modifying the primary structure of the peptide [1,21]. Unfortunately, all these approaches were accompanied by a decrease or loss of the biological activity of the peptide; thus, none of these analogues have ever reached clinical trials or were ever therapeutically applied [2].

Hence, many attempts have been made to design a proper delivery system for VIP in order to stabilize the peptide by encapsulation in, or association with, e.g. liposomes [1,22,23]. Liposomes are typically made from natural, biodegradable and non-toxic phospholipid molecules and are able to encapsulate a variety of drug molecules into their aqueous interior or to bind them into or onto their lipid membranes. Thus, all these properties make them attractive candidates for the use as drug delivery vehicles (for reviews, see [24–27]).

The pharmacokinetics of drugs can be modified by varying the liposomal composition [28]. Above that, a careful choice of the lipids is also necessary to influence the fate of the liposomes within the body. Grafting the liposomal surface with hydrophilic polymers, such as polyethylene glycol (PEG), leads to the formation of sterically stabilized liposomes, which display a longer life-time in the circulation, compared to conventional liposomes, due to a reduced recognition rate by macrophages [27,29–31].

Moreover, the association of VIP to negatively charged phospholipids induces a conformational change of the peptide from predominantly random-coiled to α-helical [5]. The latter is the preferred conformation for the ligand–receptor interaction [32,33]. Whereas, the biological activity of liposomal VIP displays no differences, irrespective, whether non-PEGylated [34] or PEGylated [23] formulations are used.

In addition, liposomes feature a great suitability as drug carriers for pulmonary administration, as they exhibit sustained drug release and depot effects. Moreover, they show aqueous compatibility and are able to prevent local drug irritation reactions in the lung [35,36]. Thereby, the PEGylation of the liposomes leads to a decreased degradation and absorption of the lipid vesicles in the lung [37]. Only recently, it was shown by Anabousi et al. [38] that PEGylation enhances the membrane integrity of the liposomes in lung surfactant and results in a lower fusion rate of the liposomes after nebulisation. Moreover, the stealth effect might reduce alveolar macrophage clearance.

Usually, the natural fate of inhaled liposomes is a transfer of their lipids to the intracellular phospholipid pool mediated by an interaction of the phospholipids with the pulmonary surfactant [17,35]. This so-called epithelial lining fluid (ELF) covers the airways, particularly the alveoli [39], and it moderates the surface tension during breathing [40]. ELF can be obtained by bronchoalveolar lavage (BAL), which is performed during fiberoptic bronchoscopy [41]. The resulting surfactant solution, called bronchoalveolar lavage fluid (BALF), is a complex mixture of cells, including alveolar macrophages, lymphocytes, bronchial epithelial cells and mast cells [39]. In addition, it contains a wide variety of soluble components, such as phospholipids (78–90%), mainly phosphatidylcholine, proteins (5–10%), which are mostly released by epithelial cells [42] and neutral lipids (4–10%), mainly cholesterol [43]. Some of these surfactant proteins as well as the neutral lipids are responsible for the adsorption of phospholipids at the air–water interface in the lung [40,44]. Besides a huge diversity of soluble proteins, BALF also contains several proteolytic enzymes, such as trypsin, cathepsin D and different carboxypeptidases [41,45].

In this study, we have investigated the stability of a liposomal drug delivery system, intended for pulmonary administration of VIP, and we have tested the integrity of liposomal-associated VIP towards proteolytic degradation. Whereas the design and physico-chemical characterization of this system is already established in our laboratory [46].

In order to mimic most closely the metabolic conditions in lung environment, the degradation behaviour of VIP

and possible changes in size and peptide load of the liposomes, were examined after incubation with the cell-free supernatant of BALF. In addition, stability experiments were conducted by incubation of the free peptide solution as well as of the liposomal-associated VIP with Krebs–Henseleit solution, a physiological buffer system, which is isoosmotic to 0.9% saline solution.

In this study, various methods were applied in order to evaluate a protective effect of liposomes towards proteolytic cleavage of VIP.

## 2. Materials and methods

Palmitoyl-oleoyl-phosphatidylcholine (POPC), lyso-stearyl-phosphatidylglycerol (lyso-PG) and polyethyleneglycol conjugated distearyl-phosphatidylethanolamine (DSPE-PEG2000) were purchased from Avanti Polar Lipids (Alabaster, AL).

VIP (amino-acid sequence HSDAVFTDNYTRLRK QMAVKKYLNSILN-NH2), N-terminally tryptophan (Trp) modified VIP (Trp-VIP) and EtCy3-VIP with the fluorescent marker Cy3 coupled to the N-terminal amino group of histidine were synthesized by piCHEM (Graz, Austria) using FMOC solid-phase peptide synthesis methodology (FMOC-SPPS). The peptides were purified by RP-HPLC.

All other chemicals were purchased from Sigma–Aldrich, Vienna, Austria.

### 2.1. Preparation of bronchoalveolar lavage fluid (BALF)

Bronchoalveolar lavage fluid (BALF) was a kind gift from the Department of Pneumology, University Hospital, and Vienna, Austria.

The lungs of the patients (10 donors) were lavaged by an instillation with a 0.9% saline solution. The resulting fluids were collected and centrifuged at 1500 rpm for 10 min in order to remove the suspending cells. Afterwards, the supernatants were pooled and stored at −20 °C.

### 2.2. Preparation of liposomes

Liposomes were prepared by thin-film rehydration method. For this purpose, stock solutions of DSPE-PEG2000, lyso-PG and POPC in pure chloroform or chloroform–methanol mixtures, respectively, were made. Aliquot amounts were mixed to obtain a molar ratio of DSPE-PEG-2000:lyso-PG:POPC of 1:7.5:11. The total lipid content of these solutions was 30 mg. The organic solvents were evaporated under a stream of nitrogen at 40 °C and vacuum desiccated overnight. The dry lipid films were hydrated in 1 mL of 10 mM Tris–HCl, pH 7.4 (Tris-buffer), each, at 40 °C for 60 min with repeated vortexing. Thereafter, the liposomal suspensions were extruded 21 times through a polycarbonate filter (Millipore, Vienna, Austria) with 100 nm pore size using a LiposoFast low pressure homogenizer (Avestin, Inc. Ottawa, ON).

Phospholipid content was quantified by a modified Bartlett inorganic phosphate assay [47].

VIP loaded liposomes (VLL) were prepared analogically to standard liposomes. Hydration was performed with peptide solution in Tris-buffer at a molar peptide to lipid ratio of 1:250.

### 2.3. Size determination

The mean diameter of the liposomes was determined by photon correlation spectroscopy (PCS) with a Zetasizer 3000 HSA (Malvern Instruments, Herrenberg, Germany). The instrument operates with a 10 mW helium–neon laser at a wavelength of 632.8 nm. The scattered light is detected at an angle of 90°. The particle size derived by an auto-correlation function is expressed as a *Z*-average, which corresponds to the mean diameter based on the intensity of scattered light.

The width of the size distribution is given in terms of the polydispersity index (PDI).

Size determination was performed after dilution to a lipid concentration of 0.03 mg/ml with buffer previously filtered through a disposable 0.02 μm membrane filter unit (Anotop 25, Whatman International Ltd., Maidstone, U.K.).

For stability experiments, the liposomal suspensions were mixed with an equal volume of Krebs–Henseleit buffer (KH-buffer), pH 7.4, containing 118 mM NaCl, 25 mM $NaHCO_3$, 2.8 mM $CaCl_2 \cdot H_2O$, 1.2 mM MgSO4, 4.7 mM KCl, 1.2 mM $KH_2PO_4$ and 2 g/l glucose or BALF and incubated at 37° for 30 min, 2 and 24 h, respectively. Thereafter, the samples were diluted as described above with buffer to a final lipid concentration of 0.03 mg/ml.

All measurements were performed at room temperature.

### 2.4. Fluorescence spectroscopy

Fluorescence of tryptophan (Trp), linked to the N-terminus of a VIP molecule (Trp-VIP), was recorded on a SPEX FLUOROMAX-3 fluorescence spectrophotometer (Jobin Yvon Horiba, Longjumeau Cedex; France). The measurements were performed using a 10 × 10 mm quartz cuvette.

The wavelength for selective excitation of tryptophan was determined at 292 nm. The emission spectra were recorded from 320 to 380 nm.

For the determination of the fluorescence of aqueous free Trp-VIP, the peptide solution was diluted with Tris-buffer, KH-buffer and BALF, respectively, to a final concentration of 10 μM.

Liposomal-associated Trp-VIP was measured directly after dilution with Tris-buffer or after incubation with BALF or KH-buffer at 37 °C for 30 min, 2 and 24 h, respectively. Anyway, the peptide concentration was 10 μM for every experiment. The experiments were performed at room temperature, except for KH-buffer and BALF incubated samples, which were measured at 37 °C.

All fluorescence values were corrected by subtracting the corresponding baseline (Tris-buffer, KH-buffer or BALF).

#### 2.4.1. Acrylamide quenching of Trp-fluorescence

To determine the accessibility of tryptophan to a water-soluble quencher, an acrylamide solution was added in increasing amounts. Its final concentration in the cuvette was in the range between 0.02 and 0.15 M.

The experiments were performed as described above and the data were analyzed with the Stern–Volmer equation.

$$\frac{I_0}{I} = K_a * [Q] + 1 \tag{1}$$

The fluorescence intensity is given by $I_0$, if no quenching solution is added and by $I$, at a given quencher concentration $Q$. $K_a$ signifies the Stern–Volmer quenching constant of the accessible fraction. All data were corrected for background and volume increase.

For the calculation of the Stern–Volmer quenching constants, intensity values were taken at the wavelength of the respective emission maximum, which was different for free and liposomal-associated Trp-VIP.

### 2.5. Fluorescence fluctuation spectroscopy

Stability of liposomes and especially short-term release of VIP at relatively low concentration was measured with Fluorescence Fluctuation Spectroscopy (FFS). FFS provides detailed information about dynamics, concentration, size and brightness of fluorescent entities [48–50]. In our case, FFS represents the combination of Fluorescence Correlation Spectroscopy (FCS) [51] and Fluorescence Intensity Distribution Analysis (FIDA) [52] of Photon Counting Histograms (PCH) [49,53]. These techniques use the diffusion of fluorescent particles through a small ($V = 1$ fL) and defined focus element to extract their number, diffusion dynamics and brightness.

#### 2.5.1. FFS measurements

A confocal microscope (Confocor1-Carl Zeiss, Jena, Germany) was used to measure dynamics of both free and liposomal-associated EtCy3-VIP.

Samples were excited with the 543 nm laser line of a He/Ne laser (Uniphase, USA). The confocal pinhole diameter was set to 45 μm and calibrated with rhodamine B. FFS measurements were performed in aqua bidest, KH-buffer and BALF, respectively, at a final VIP concentration of 250 nM.

#### 2.5.2. FCS analysis

Fluorescence signals were detected for 10 s with 0.5 s interval with an auto-correlator card (ALV-5000/E). The auto-correlation curves were fitted with an auto-fitting routine, developed in python programming language using the auto-correlation function [54]:

$$G(\tau) = \frac{\langle \delta I(t)\delta I(t-\tau)\rangle}{\langle \delta I(t)\rangle^2} = 1 + \frac{1}{N}\sum_{i=1\ldots3}\frac{F_i}{(1+\frac{\tau}{\tau_i})}\frac{1}{\sqrt{(1+\frac{\tau}{SP^2\tau_i})}} \tag{2}$$

The term δI denotes the intensity fluctuations from the temporal average. $F_i$ and $\tau_I$ represent the fraction and diffusion time of the component $I$, and $N$ stands for the number of particles in the focus element, which correlates to the concentration in the observed medium. SP represents the relation of the two axes of the focal element.

#### 2.5.3. FIDA analysis

Fluorescence signals were detected continuously using a Time Measurement Histogram Accumulation Real-Time Processor (Time Harp 200, PicoQuant, Germany) triggered with 7.4 MHz. Raw data were histogrammed and normalized by area. The resulting PCHs were fitted to the FIDA model using a Levenberg-Marquart algorithm. The model works in Fourier space using the generating function [55]. The probability distribution by a given bin-time ($t_{bin}$) is retrieved by an inverse Fourier transformation:

$$P(n, t_{bin}) = FFT^{-1}G(\zeta, t_{bin}) = FFT^{-1}\exp\left[(\zeta-1)\lambda t_{bin} + \sum_s c_s \int_V e^{\{[(\zeta-1)q_w t_{bin}B(r)]-1\}}dV\right] \tag{3}$$

Here, $c_s$ relates to the concentration and $q_w$ accounts for the specific brightness of different particles ($s$). The term $\lambda$ is a parameter for the background noise and $B(r)$ represents the spatial brightness distribution in the focal volume ($V$).

### 2.6. High performance liquid chromatography (HPLC)

Reverse-phase HPLC was performed on a Hewlett-Packard-Agilent liquid chromatograph, series 1100 (Hewlett-Packard, Waldborn, Germany), equipped with a Vydac $C_{18}$ column (218TP5215; Vydac, Hesperia, CA) with 5 μm particle size, 30 nm pore size, a length of 150 mm and a diameter of 2.1 mm.

An aqueous VIP solution as well as VLL were eluted from the column with a gradient of water and acetonitrile with 0.1% (v/v) trifluoroacetic acid (TFA) [0–90% (v/v) acetonitrile in 15 min] with detection by UV absorption at 215 nm.

The final concentration of water and acetonitrile was retained for five more minutes.

The flow rate was 0.5 ml/min. All fractions were collected in Eppendorff tubes and subjected to MS analysis.

For digest experiments, free VIP and VLL were mixed with an equal volume of BALF and incubated at 37 °C. To investigate the level of degradation, aliquots of these solutions were injected into the HPLC column immediately after mixing, and after 2 and 24 h of incubation. The separation conditions were as described above.

Again, the fractions were collected manually and subjected to MS analysis.

### 2.7. Mass spectrometry (MS)

Matrix-assisted laser desorption/ionization-time of flight (MALDI-TOF) mass spectra were obtained in positive linear mode on an Axima CFR mass spectrometer (KRATOS, Manchester, UK) by integrating 20–50 laser shots per spectrum.

As a matrix, alpha-cyano-4-hydroxycinnamate saturated in 30% (v/v) acetonitrile and 0.1% (v/v) TFA in water was used.

External calibration was performed with a mixture of adrenocorticotropic hormone (ACTH) fragment 18–39 ($MH^+$ 2466.71) and insulin ($MH^+$ 5733.5).

### 2.8. Effects of liposomal VIP on rat lung arteries in vitro

Pulmonary arteries were extracted from adult male Sprague–Dawley rats (Abteilung für Labortierkunde und Labortiergenetik, Medical University of Vienna, Himberg, Austria). The lungs of the animals were removed subsequently after anesthetization. The pulmonary arterial tree was rapidly dissected from the lung parenchyma. The arteries, which were opened longitudinally, were cut into zigzag strips with approximately 1.3–1.5 cm length. After mounting these strips in an organ bath, which contained 9 ml of KH-buffer (pH 7.4) gassed with 95% O2 and 5% CO2, they were equilibrated for 2–3 h.

Activity measurements of the arterial strips took place isotonically under a resting load of 1 g. Extension and contraction of the arteries were translated into mechanical signals, processed by bridge amplifiers (Hugo Sachs Elektronik, Germany) and recorded on ink writers.

For the determination of the vasodilatory effect of VIP, the arteries were precontracted with L-phenylephrine hydrochloride (Phe; 0.1 μM) and subsequently exposed to 100 nM free or liposomal VIP. Thereafter, the relaxation efficiency and the time period to attain the maximal relaxation were recorded.

In order to check the stability of the peptide as well as its vasodilatory properties, free VIP and VLL were mixed with BALF and incubated at 37 °C. Aliquots of these solutions were taken after 0, 1, 2.5, 5, 10, 15, 30, 60 and 90 min and studied in the arterial experiment at the same conditions as described above

To control the retained viability of the arterial strips, the arteries were treated with acetylcholine (1 μM) at the end of each experiment and regarded as intact, if they show more than 60% relaxation of the Phe-induced precontraction.

Arterial experiments using blank liposomes displayed that liposomes themselves have no influence on the precontraction or relaxation behaviour of the lung arteries.

### 2.9. Data and statistical analysis

Data are expressed as means ± SEM. The number of independent experiments is given as $n$.

For the statistical evaluation a 2-sample $t$-test was used. Statistical significance was assumed at $p < 0.05$. Statistics were performed using the program MINITAB 13.31 (MinTab Inc.)

## 3. Results and discussion

Recently, we have reported on a VIP loaded liposomal formulation, which is intended for the pulmonary application of VIP [46].

Here, we investigate the susceptibility of free and liposomal VIP towards enzymatic degradation, which rapidly occurs in the lung (for a review see [4]), and we address the question whether liposomal-associated VIP is thus protected from proteolytic digestion. To mimic the conditions after pulmonary administration, solutions of free VIP as well as empty and VIP loaded liposomes were investigated in a metabolic environment, which was simulated by either a physiological buffer system (KH-buffer) or the cell-free supernatant of BALF. BALF contains numerous digestive proteases including trypsin, cathepsin D and several carboxypeptidases, which are responsible for the rapid cleavage of the peptide in the lung [39,41,45].

### 3.1. Liposomal size stability

The unilamellar, sterically stabilized liposomes, consisting of a ternary mixture of lipids, were prepared by thin-film rehydration method as described earlier [46]. Thereafter, the liposomal suspensions were extruded in order to enhance the homogeneity of the size distribution, expressed by a low polydispersity index (PDI) of the PCS data, and to facilitate the comparability of diameter values.

A mean particle diameter of 95 ± 2 nm and a PDI < 0.1 were obtained for freshly prepared extruded liposomes in Tris-buffer ($n = 7$). Incubation of the liposomal formulation with KH-buffer ($n = 3$) and BALF ($n = 3$) at 37 °C for 30 min, 2 and 24 h, had no significant influence ($p$-values $\geqslant 0.2$) on the particle size as shown in Table 1.

As published previously [46], the mean diameter of the liposomes is not affected by VIP loading. This also applied for those VLL, which were hydrated with Trp-VIP and EtCy3-VIP (data not shown).

### 3.2. Peptide–lipid association in different media

The sensitivity of the fluorescence emission maximum of the Trp residue in Trp-VIP to its environment allows to monitor the association of Trp-VIP to liposomes in different media. The fact that VIP becomes associated with the negatively charged bilayer of the liposomes is demonstrated by a pronounced blue-shift in the tryptophan fluorescence emission maximum as compared to the emission maximum for free Trp-VIP in Tris-buffer (blue-shift from 355 to 334 nm). In order to test if the association between the peptide and the lipid membrane is retained after an incubation of 30 min at 37 °C with KH-buffer and BALF,

Table 1
Size and PDI values of KH-buffer and BALF incubated liposomes after 0.5, 2 and 24 h of incubation

| Incubation time [h] | KH-buffer | | BALF | |
|---|---|---|---|---|
| | Mean diameter ± SEM [nm] | PDI ± SEM | Mean diameter ± SEM [nm] | PDI ± SEM |
| 0.5 | 100 ± 3 | 0.15 ± 0.09 | 96 ± 3 | 0.18 ± 0.15 |
| 2 | 99 ± 1 | 0.15 ± 0.08 | 104 ± 1 | 0.17 ± 0.09 |
| 4 | 95 ± 2 | 0.15 ± 0.11 | 100 ± 2 | 0.28 ± 0.04 |

Each value is the mean calculated from 3 separate preparations and the standard error of the mean is presented.

respectively, the corresponding fluorescence spectra were recorded. Fig. 1A shows that the blue-shift of the fluorescence emission maximum of Trp is preserved for KH-buffer and BALF incubated Trp-VIP liposomes. Data of free and liposomal-associated Trp-VIP in Tris-buffer were also replotted as a control. To investigate the long-term integrity, Trp-VIP liposomes were incubated with KH-buffer and BALF for 2 and 24 h. Again, we found a preserved blue-shift for all samples, indicating a maintained association between the peptide and the lipid vesicles (data not shown).

Apart from the blue-shift, the low accessibility of Trp in Trp-VIP loaded liposomes to a water-soluble quencher, namely acrylamide, is a second parameter to assess the association of the peptide with the lipid membrane. We have already shown that the Stern–Volmer constants for free Trp-VIP ($Ka = 20.1\ M^{-1}$) and liposomal-associated Trp-VIP in Tris-buffer ($Ka = 1.8\ M^{-1}$) are significantly different [46]. By analogy, Fig. 1B depicts the Stern–Volmer plot of acrylamide quenching for liposomal Trp-VIP in different incubation media in comparison to free VIP in Tris-buffer. As clearly seen in the figure, acrylamide added to free VIP in buffer shows a significantly higher quenching efficiency. According to Eq. (1), the Stern–Volmer constants were calculated, resulting in $1.4\ M^{-1}$ and $1.8\ M^{-1}$ for KH-buffer and BALF incubated liposomes, respectively. Similarly, Ka was $1.5\ M^{-1}$ for Trp-VIP liposomes, incubated with KH-buffer for 2 h, and this value remained unchanged for those liposomes incubated for 24 h. Likewise, the calculated constants for BALF incubated Trp-VIP liposomes after 2 and 24 h of incubation displayed no difference, being $Ka = 1.6\ M^{-1}$.

Hence, the quenching profiles of Trp by acrylamide, which are indicative for the accessibility of Trp, clearly demonstrate that incubation with KH-buffer or BALF had no effect on the local environment of the Trp residue, being still associated with the lipid bilayer, whereas no apparent release or dissociation of the peptide from the liposome can be deduced. Thus, we hypothesize that VIP association to liposomes exhibits a strong resistance to proteolytic degradation mediated by enzymes present in BALF. This may simply arise from the fact that the lipid bilayer is not permeable for enzymes [5]. Nevertheless, as the association of positively charged VIP to the negatively charged phospholipids is driven by electrostatics, we assume that during hydration VIP becomes not exclusively encapsulated in the aqueous interior of the liposomes, but that it is associated to the inner and outer leaflet of the lipid membrane. Accordingly, a part of the peptide is basically not accessible to the enzymes in BALF, as long as the liposomes stay integer in this fluid. Whereas the remaining part of the VIP molecules, which is attached to the outer leaflet of the membrane, is not shielded by the bilayer, even so these molecules resist enzymatic cleavage. One explanation could be that most of the peptide bonds cleaved by enzymes are located in the central segment of VIP, the region with the highest propensity for amphipathic helix formation [56]. Indeed, a conformational change of VIP from predominantly random coil in aqueous solution to α-helical in the presence of negatively charged phospholipids is reported by several groups [5,33]. Consistently, we found a significantly increased helicity for VIP associated to our liposomes [46]. In this context, it was hypothesized by Gololobov et al. [5] that an efficient binding of degrading enzymes to VIP requires a conformational flexibility in the central region of the peptide, which is not given due to the stabilization of the α-helix by anionic lipids, resulting in a limited recognition by the catalyst.

Another aspect concerns the grafting of the liposomal surface with polyethylene glycol leading to the formation of a protective shell, which exhibits an additional hydration shield by the association of water molecules [57]. PEGylated proteins, for instance, display an enhanced resistance to degradation by proteolytic enzymes, such as trypsin and chymotrypsin [57–59]. Therefore, it can be assumed that VIP, associated to sterically stabilized liposomes, is to some extent shielded from enzymatic cleavage, due to the protective shell of PEG molecules. Thereby, this steric hindrance results in a reduced accessibility of the peptide molecules to different enzymes.

The data obtained from Trp-fluorescence were further supported by the results derived from FFS. In Fig. 2A, a compilation of the FFS measurements of native EtCy3, EtCy3-VIP and EtCy3-VIP loaded liposomes in KH-buffer and BALF is presented. The FCS measurements in KH-buffer (A1) and BALF (A2) clearly display discriminable diffusion times ($\tau$) for EtCy3 (green), EtCy3-VIP (red) and EtCy3-VIP liposomes (black). The PCH curves extracted from the measurements in KH-buffer (B1) and BALF (B2) show good accordance between native EtCy3 (green) and EtCy3-VIP (red) in respect to the specific brightness (Q). Only a minute amount of particles exhibit a higher specific brightness (arrow). Small differences in brightness might be caused by aggregation or changes in the quantum yield of EtCy3 in different environments. In

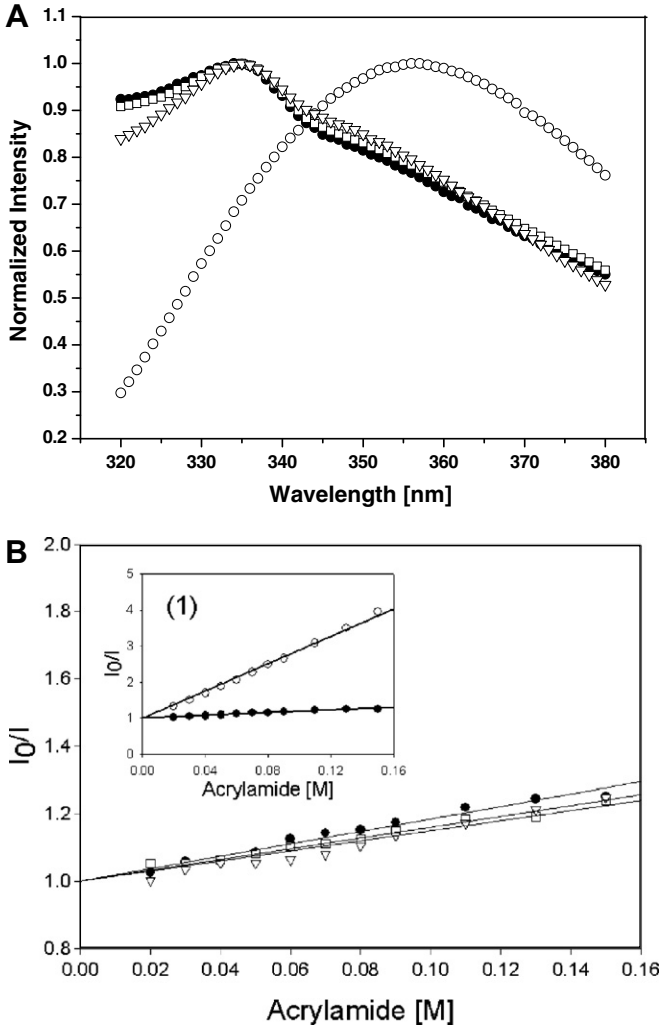


Fig. 1. (A) Fluorescence emission spectra for free and liposomal-associated Trp-VIP in different media. The spectra are shown as a function of normalized intensities. The emission intensity maximum for free Trp-VIP in Tris-buffer (○) arose at 355 nm and was shifted to a shorter wavelength for liposomal-associated Trp-VIP (●) in Tris-buffer. After incubation of Trp-VIP liposomes for 30 min at 37 °C with KH-buffer (□) or with BALF (▽), the blue-shift of the maximum to 334 nm, indicative for liposomal association, is still preserved. (B) Stern–Volmer plot of the acrylamide quenching data of liposomal Trp-VIP in Tris-buffer (●) and after incubation with KH-buffer (□) and BALF (▽), respectively. The acrylamide concentration was varied between 0.02 and 0.15 M. For the calculation of the Stern–Volmer constant, intensity values were taken at the emission maximum of liposomal Trp-VIP (334 nm). The insert displays the Stern–Volmer plot for free Trp-VIP (○) and liposomal Trp-VIP in Tris-buffer (●). The intensity values were taken at the wavelength of the respective emission maximum, for free (355 nm) and liposomal Trp-VIP (334 nm).

contrast, EtCy3-VIP liposomes (black) feature high specific brightness values, indicated by the right shift of the PCH curve. The detailed analysis of the FCS and PCH curves is presented in the following paragraph and a summary of the FFS measurements is given in Table 2.

For EtCy3-VIP, a diffusion time of ~115 μs was detected in all media (aqua bidest, KH-buffer and BALF), in which the values agree within the error limits. Additionally, for a smaller fraction of particles a higher diffusion time of 240 ± 20 μs was observed in aqua bidest, which might be caused by aggregation of the hydrophobic peptide. This slow component was not found in BALF or KH-buffer, probably because the aggregation tendency is reduced by the ionic strengths of these media.

As expected for BALF, an additional smaller diffusion time of about 65 ± 10 μs is observed. This diffusion time, which is representative for a fast species in solution, is most probably the result of the proteolytic activity of BALF. However, this diffusion time is still somewhat slower than for free EtCy3, which shows a τ-value of 35 ± 5 μs. Despite different diffusion times, all EtCy3-VIP entities show similar brightness values in BALF. This corresponds to the appearance of various species of different sizes, but labelled with one dye molecule and most likely results from proteolytic fragments of EtCy3-VIP, as already suspected above. Similar to EtCy3-VIP, free EtCy3 indicates brightness values of 3–4 kHz for the native dye in all media. Only in aqua bidest a brighter species was observed, showing also a slower diffusion time.

For liposomes in aqua bidest, KH-buffer and BALF, the majority of fluorescent entities show diffusion times around 1.3 ms, which correspond within the error limits to single liposomes loaded with EtCy3-VIP. This is in agreement with a particle size of about 100 nm, as obtained by dynamic light scattering (see above). For 10–15% of the observed entities in aqua bidest and KH-buffer smaller diffusion times are detected and might represent aggregates of peptides or of peptides with lipids.

In BALF, a minor population of faster particles was observed representing the two species found for EtCy3-VIP in BALF, i.e. free EtCy3-VIP and proteolysis products. The concentration analysis of the liposomes in BALF (see Fig. 2B) shows a slight increase of the percentage of the fast component (+0.3%/min) with observation time (Fig. 2B, insert A, black line); however, the total concentration of the fast component does not exceed 20% even after 60 min. In addition, this fast component features a very inhomogeneous size distribution, which is reflected by a broad distribution of diffusion times (Fig. 2B, insert B, red).

In contrast, liposomes in KH-buffer show a decrease in the percentage of the faster component by −0.10%/min (Fig. 2B, insert A, blue line). This decrease might be caused by a hydrophobic interaction with the sample well, as a corresponding decrease in concentration is also observed for free EtCy3-VIP in KH-buffer or aqua bidest (data not presented).

FIDA showed that EtCy3-VIP loaded liposomes in KH-buffer and BALF have a 50- to 100-fold higher brightness, compared to free EtCy3-VIP, which indicates about 75 ± 25 EtCy3-VIP molecules per liposome. Liposomes in aqua bidest have a higher specific brightness indicating a slightly higher EtCy3-VIP concentration per liposome. This might result from some unspecific aggregation of EtCy3-VIP molecules on the surface of the liposomes.

The number of EtCy3-VIP molecules per liposome obtained from these data is somewhat smaller than the values calculated from the chemical composition and liposomal size, estimated to about 200. Nevertheless, FIDA values depend critically on the determination of the fluorescence quantum yield for EtCy3 in different environment,

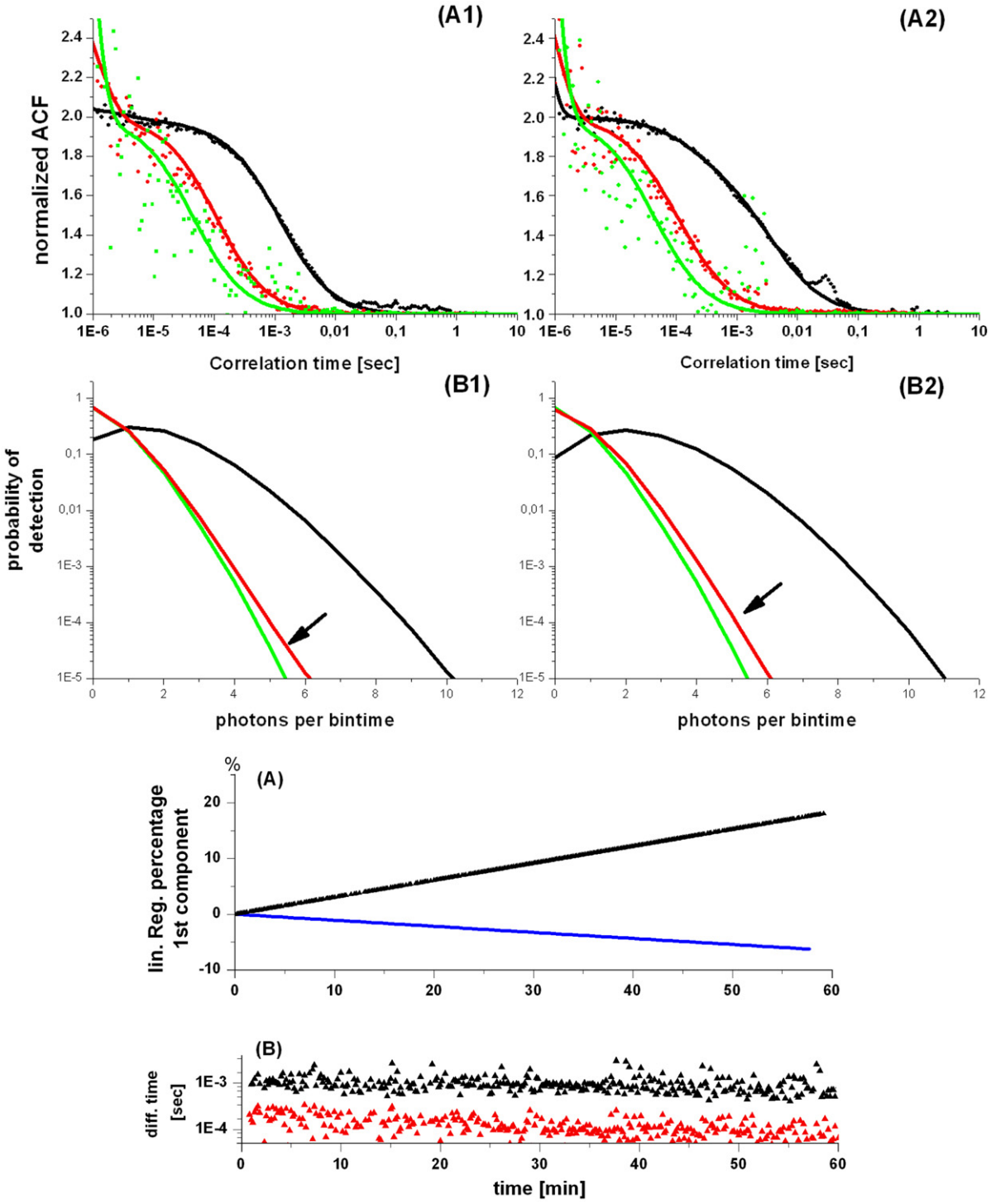


Fig. 2. Compilation of FFS measurements. Normalized FCS curves (dots) and fits (lines) of EtCy3 (green), EtCy3-VIP (red) and EtCy3-VIP loaded liposomes (black) in KH-buffer (A1) and BALF (A2) are shown together with PCH curves of EtCy3 (green), EtCy3-VIP (red) and EtCy3-VIP loaded liposomes (black) in KH-buffer (B1) and BALF (B2). The arrows indicate the species of slightly increased brightness. Concentration analysis of the FFS results for EtCy3-VIP loaded liposomes in different media. (A) Linear regression of the percentage of the fast diffusing component of liposomes in BALF (black) and KH-buffer (blue). (B) Time dependent diffusion time development of liposomes in BALF (black – slow diffusing component; red – fast diffusing component). (For interpretation of the references in colour in this figure legend, the reader is referred to the web version of this article.)

Table 2
FFS analysis of free EtCy3-VIP and EtCy3-VIP loaded liposomes in different media

| Media | EtCy3-VIP | | | | EtCy3-VIP loaded liposomes | | | |
|---|---|---|---|---|---|---|---|---|
| | $\tau_1$ [μs] | $Q_1$ [kHz] | $\tau_2$ [ms] | $Q_2$ [kHz] | $\tau_1$ [μs] | $Q_1$ [kHz] | $\tau_2$ [μs] | $Q_2$ [kHz] |
| Aqua | 110 ± 10 | 3 ± 1 | 240 ± 20 | 7 ± 4 | 155 ± 20 | 4 ± 2 | 1.3 ± 0.4 | 400 ± 200 |
| KH | 115 ± 12 | 3 ± 1 | | | 160 ± 15 | 6 ± 2 | 1.2 ± 0.2 | 350 ± 100 |
| BALF | 65 ± 10 | 4 ± 1 | 120 ± 10 | 4 ± 1 | 100 ± 20 | 6 ± 1 | 1.5 ± 0.5 | 300 ± 100 |

$\tau_1$ and $Q_1$ are the diffusion time and brightness of the faster species; $\tau_2$ and $Q_2$ are the diffusion time and brightness of the slower species.

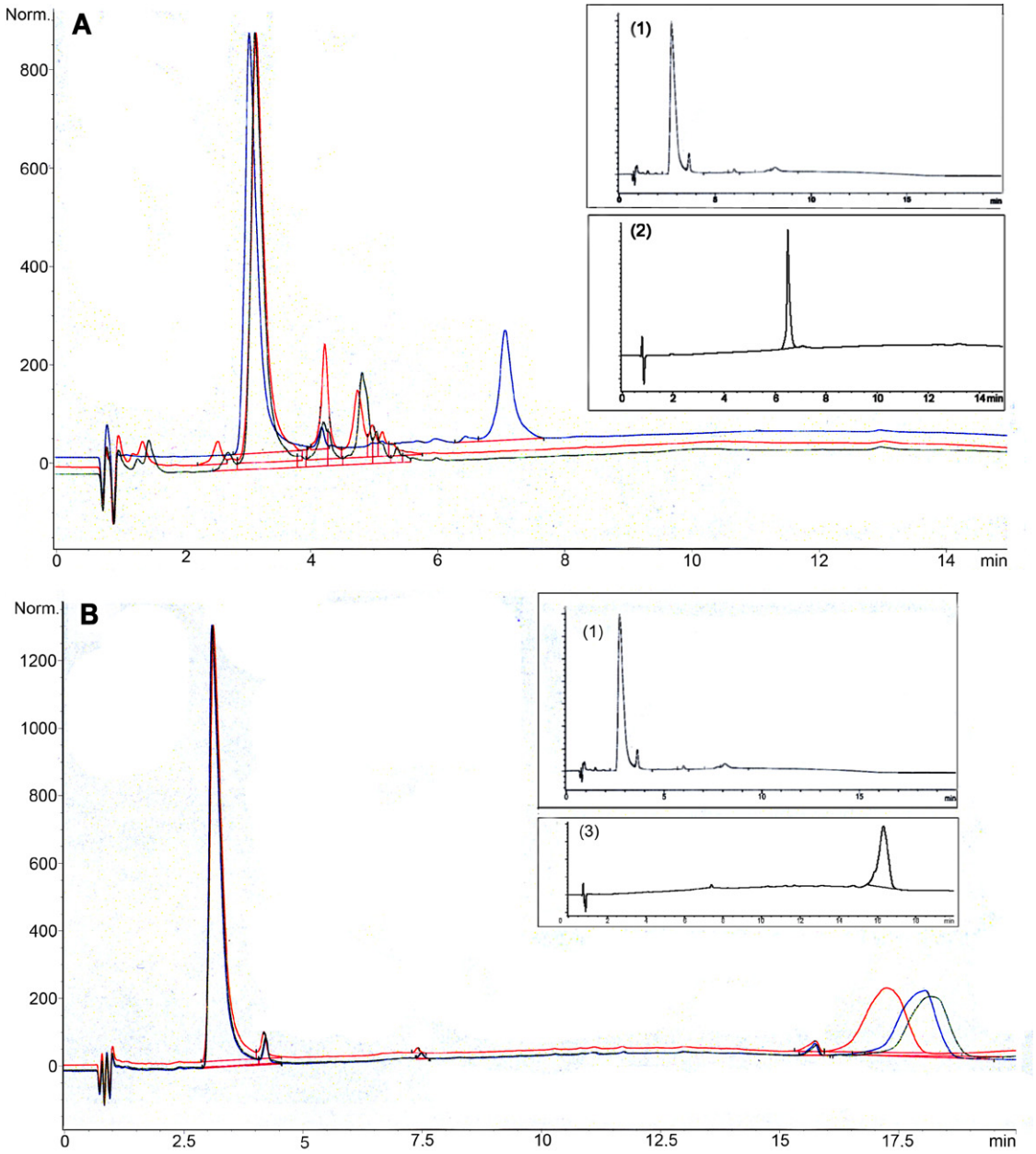


Fig. 3. (A) HPLC chromatogram of free VIP with BALF. The red line shows the chromatogram of VIP, subsequently after mixing with BALF. The green and the blue lines display the chromatogram after 2 and 24 h of incubation with BALF at 37 °C, respectively. Insert (1) reveals the curve of BALF and insert (2) shows the single peak of free VIP in buffer. The chromatograms are normalized to the strongest peak intensity. (B) HPLC chromatogram of liposomal VIP with BALF. According to (A), the red curve shows the chromatogram, received immediately after mixing VLL with an equal volume of BALF. The green and the blue lines were obtained after 2 and 24 h of incubation with BALF at 37 °C, respectively. The chromatograms are normalized to the strongest peak intensity. Inserts (1) and (3) are the curves for pure BALF and VLL in buffer, respectively. (For interpretation of the references in colour in this figure legend, the reader is referred to the web version of this article.)

and a minute amount of free EtCy3-VIP was found in all preparations. To summarize, EtCy3-VIP loaded liposomes showed a high stability in all tested media. In BALF, the EtCy3-VIP molecule becomes definitely cleaved, whereas only minor cleaved products were obtained for liposomal protected EtCy3-VIP.

### 3.3. Digest studies and cleavage products

To identify and quantify free and liposomal VIP and cleavage products thereof after incubation with BALF, RP-HPLC and MS were used. Free and liposomal VIP were easily distinguishable in the HPLC chromatogram by their retention time. Free VIP (Insert 2 shown in Fig. 3A) eluted after 6.5 min, whereas liposomal-associated VIP (Insert 3 shown in Fig. 3B) was detected after 16.3 min. As a reference for digest samples, BALF (Insert 1 shown in Fig. 3A and 3B) was injected to the HPLC. It showed two characteristic peaks with retention times of 2.7 and 3.6 min.

Figs. 3A and B show the chromatograms of free VIP and VLL, respectively, immediately after mixing with BALF (red curve) and after incubation at 37° for 2 h (green curve) and 24 h (blue curve).

The single peak of aqueous VIP was exclusively found immediately after mixing with BALF. Longer incubation times resulted in a pronounced cleavage of the peptide, marked by the appearance of additional peaks in the chromatogram (see Fig. 3A). Accordingly, the characteristic mass of 3326.8 Da (native VIP) was only found immediately after mixing with BALF. The different molecular masses determined for the cleavage products after 2 and 24 h of incubation are summarized in Table 3 and are correlated to VIP fragments, as shown in Table 4.

Thus, as expected, free VIP was completely cleaved, while prone to the enzymes in BALF. We assume that after specific cleavage of peptide bonds by NEP [4], the peptide fragments are freely accessible to exopeptidases resulting in rapid, complete degradation of VIP and in the formation of more unspecific products. In keeping with these results, similar cleavage products were also obtained for limited proteolysis of VIP with trypsin and thermolysin [60].

In contrast to free VIP, the single peak obtained for liposomal-associated VIP remained almost unaffected by BALF, even after 24 h of incubation (Fig. 3B). Consistently, only the molecular mass of intact VIP was found by MS. Clearly, retention times and masses of 15.8 min (3327 Da), 17.2 min (3326 Da) and 18.1 min (3325 Da) were found for incubation times of 0, 2 and 24 h, respectively.

Table 4
Masses for VIP fragments and corresponding amino acid sequences

| Molecular mass [Da] | Proteolytic fragments | Amino acid sequence |
|---|---|---|
| 1425.5 | VIP(1–12) | HSDAVFTDNYTR |
| 1425.6 | VIP(7–17) | TDNYTRLRKQM |
| 1823.0 | VIP(1–15) | HSDAVFTDNYTRLRK |
| 1951.1 | VIP(1–16) | HSDAVFTDNYTRLRKQ |
| 1949.4 | VIP(11–26) | TRLRKQMAVKKYLNSI |
| 1694.8 | VIP(1–14) | HSDAVFTDNYTRLR |
| 1611.8 | VIP(4–16) | AVFTDNYTRLRKQ |

### 3.4. Vasoreactivity of VIP after BALF incubation

Once cleaved, VIP loses its biological activity [20]. Here, we have tested in an *ex vivo* arterial model system if liposomes are able to conserve the dilatory efficiency of VIP even after exposure to BALF. In a first step, the vasorelaxation efficiency of free VIP in Tris-buffer and in BALF, respectively, expressed as percent of maximal relaxation of precontracted arteries, was determined. The same test series were performed for VIP loaded liposomes. The results are summarized in Fig. 4 showing the maximal relaxation efficiency for free and liposomal VIP as a function of incubation time in BALF. Control experiments performed in the absence of BALF revealed relaxation values of about 45% and 35% of the precontraction for free VIP and VLL, respectively. After 1 min of incubation with BALF, free VIP loses over 50% of its relaxation efficiency (contraction change from $-43.4 \pm 2.0$ to $-20.3 \pm 4.8\%$, $n = 6$). A further decrease to about 12% is observed after 2.5 min. For 5–90 min of incubation the relaxation values remained almost constant varying between 3% and 7%, indicating a complete loss of relaxation efficiency. This behaviour can easily be ascribed to a breakdown of VIP due to enzymatic cleavage.

In contrast, liposomal VIP, which exerts a maximal relaxation efficiency of $34.1 \pm 3.5\%$ in Tris-buffer, showed less response to BALF incubation. After 1 min of incuba-

Table 3
Mass values of VIP fragments separated by HPLC after incubation for 0, 2 and 24 h with BALF

| Incubation: 0 min | | Incubation: 2 h | | Incubation: 24 h | |
|---|---|---|---|---|---|
| Retention time [min] | Mass [Da] | Retention time [min] | Mass [Da] | Retention time [min] | Mass [Da] |
| 6.0 | 3324 | 4.2 | 1427 | 4.2 | 1426 |
| – | – | 4.7 | 1826 | 4.8 | 1824 |
| | | | 1952 | | 1952 |
| – | – | 5.1 | 1695 | 5.0 | 1695 |
| – | – | 5.3 | 1828 | 5.3 | 1827 |
| – | – | – | – | 5.4 | 1763 |
| – | – | – | – | 5.9 | 1608 |

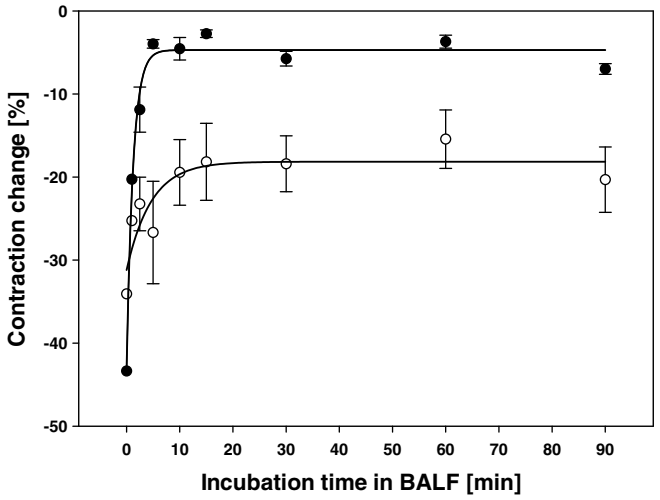


Fig. 4. Vasorelaxation efficiency of free VIP (●) and liposomal-associated VIP (○) after incubation with BALF. The incubation time was varied between 0 and 90 min. The relaxation efficiency is expressed as % contraction change from phenylephrine-induced precontraction taken as 0%. Each point represents the means ± SEM ($n$, at least 6 independent experiments).

tion the relaxation value was changed to $25.3 \pm 3.9\%$ ($n = 8$) and remained almost unchanged for longer incubation periods, varying between 16% and 27% vasorelaxation activity.

According to these data, an incubation of VIP with this catalytic fluid results in a complete loss of biological activity, if VIP is not protected by liposomes. From a direct comparison of the biological efficiencies of free and liposomal VIP after defined incubation periods in BALF, it becomes evident that the vasodilatation properties of the peptide are in large part preserved, when associated to the lipid membrane.

## 4. Conclusion

In the present study, we have tested a liposomal drug delivery system, intended for the pulmonary administration of VIP, a cationic vasodilatory peptide that is highly sensitive to enzymatic degradation in the lung environment. We could demonstrate the stability of the unilamellar liposomes in respect of size and drug load efficiency under metabolic conditions, mimicked by BALF. Moreover, the protective role of liposomes on proteolytic cleavage of VIP was shown by fluorescence techniques. Equally, the biological activity of VIP was largely preserved by liposomes.

In conclusion, our data provide strong experimental evidence that sterically stabilized liposomal formulations have the potential to enhance the life-time and biological activity of peptide drugs in the metabolic environment of the lung.

## Acknowledgements

The Austrian Nano-Initiative co-financed this work as part of the Nano-Health (Project No. 0200), the sub-projects NANO-LIPO, NANO-BREATH, NANO-FLU being financed by the Austrian FWF (Fonds zur Förderung der Wissenschaftlichen Forschung) (Project Nos. N202, N206, N209) and NANO-VIP by the FFF (Project No. 253-NAN).

We are grateful to Bernadette Zanner and Dorina Clay for technical assistance.

## References

[1] E. Refai, C. Jonsson, M. Andersson, H. Jacobsson, S. Larsson, P. Kogner, M. Hassan, Biodistribution of liposomal 131I-VIP in rat using gamma camera, Nucl. Med. Biol. 26 (1999) 931–936.
[2] V. Sethi, H. Onyuksel, I. Rubinstein, Liposomal vasoactive intestinal peptide, Methods Enzymol. 391 (2005) 377–395.
[3] D.A. Groneberg, K.F. Rabe, U. Wagner, A. Fischer, Vasoactive intestinal polypeptide in the respiratory tract: physiology and pathophysiology, Pneumologie 58 (2004) 330–338.
[4] D.A. Groneberg, K.F. Rabe, A. Fischer, Novel concepts of neuropeptide-based drug therapy: vasoactive intestinal polypeptide and its receptors, Eur. J. Pharmacol. 533 (2006) 182–194.
[5] G. Gololobov, Y. Noda, S. Sherman, I. Rubinstein, J. Baranowska-Kortylewicz, S. Paul, Stabilization of vasoactive intestinal peptide by lipids, J. Pharmacol. Exp. Ther. 285 (1998) 753–758.
[6] V. Petkov, W. Mosgoeller, R. Ziesche, M. Raderer, L. Stiebellehner, K. Vonbank, G.C. Funk, G. Hamilton, C. Novotny, B. Burian, L.H. Block, Vasoactive intestinal peptide as a new drug for treatment of primary pulmonary hypertension, J. Clin. Invest. 111 (2003) 1339–1346.
[7] X.P. Gao, Y. Noda, I. Rubinstein, S. Paul, Vasoactive intestinal peptide encapsulated in liposomes: effects on systemic arterial blood pressure, Life Sci. 54 (1994) 247–252.
[8] D. Ganea, M. Delgado, Vasoactive intestinal peptide (VIP) and pituitary adenylate cyclase-activating polypeptide (PACAP) as modulators of both innate and adaptive immunity, Crit. Rev. Oral. Biol. Med. 13 (2002) 229–237.
[9] A. Dejda, P. Sokolowska, J.Z. Nowak, Neuroprotective potential of three neuropeptides PACAP, VIP and PHI, Pharmacol. Rep. 57 (2005) 307–320.
[10] S. Ollerenshaw, D. Jarvis, A. Woolcock, C. Sullivan, T. Scheibner, Absence of immunoreactive vasoactive intestinal polypeptide in tissue from the lungs of patients with asthma, N. Engl. J. Med. 320 (1989) 1244–1248.
[11] C. Surrenti, D. Renzi, M.R. Garcea, E. Surrenti, G. Salvadori, Colonic vasoactive intestinal polypeptide in ulcerative colitis, J. Physiol. Paris 87 (1993) 307–311.
[12] P. Dorfmuller, F. Perros, K. Balabanian, M. Humbert, Inflammation in pulmonary arterial hypertension, Eur. Respir. J. 22 (2003) 358–363.
[13] G.G. Pietra, The Pathology of Primary Pulmonary Hypertension, in: L.J. Rubin, S. Rich (Eds.), Primary Pulmonary Hypertension, Marcel Dekker, New York, 1997, pp. 19–61.
[14] E.K. Tam, G.M. Franconi, J.A. Nadel, G.H. Caughey, Protease inhibitors potentiate smooth muscle relaxation induced by vasoactive intestinal peptide in isolated human bronchi, Am. J. Respir. Cell Mol. Biol. 2 (1990) 449–452.
[15] E.K. Tam, G.H. Caughey, Degradation of airway neuropeptides by human lung tryptase, Am. J. Respir. Cell Mol. Biol. 3 (1990) 27–32.
[16] K.M.G. Taylor, S.J. Farr, Liposomes for pulmonary drug delivery, in: G. Gregoriadis, A.T. Florence, H.M. Patel (Eds.), Liposomes in Drug Delivery, Harwood Academic Publishers, Chur, 1993, pp. 95–110.
[17] R. Mitra, I. Pezron, Y. Li, A.K. Mitra, Enhanced pulmonary delivery of insulin by lung lavage fluid and phospholipids, Int. J. Pharm. 217 (2001) 25–31.
[18] H. Suzuki, X.P. Gao, C.O. Olopade, I. Rubinstein, Neutral endopeptidase modulates VIP-induced vasodilation in hamster cheek pouch vessels in situ, Am. J. Physiol. 271 (1996) 393–397.

[19] E.J. Goetzl, S.P. Sreedharan, C.W. Turck, R. Bridenbaugh, B. Malfroy, Preferential cleavage of amino- and carboxyl-terminal oligopeptides from vasoactive intestinal polypeptide by human recombinant enkephalinase (neutral endopeptidase, EC 3.4.24.11), Biochem. Biophys. Res. Commun. 158 (1989) 850–854.
[20] C.M. Lilly, J.M. Drazen, S.A. Shore, Peptidase modulation of airway effects of neuropeptides, Proc. Soc. Exp. Biol. Med. 203 (1993) 388–404.
[21] D.R. Bolin, J. Michalewsky, M.A. Wasserman, M. O'Donnell, Design and development of a vasoactive intestinal peptide analog as a novel therapeutic for bronchial asthma, Biopolymers 37 (1995) 57–66.
[22] H. Ikezaki, S. Paul, H. Alkan-Onyuksel, M. Patel, X.P. Gao, I. Rubinstein, Vasodilation elicited by liposomal VIP is unimpeded by anti-VIP antibody in hamster cheek pouch, Am. J. Physiol. 275 (1998) 56–62.
[23] F. Sejourne, I. Rubinstein, H. Suzuki, H. Alkan-Onyuksel, Development of a novel bioactive formulation of vasoactive intestinal peptide in sterically stabilized liposomes, Pharm. Res. 14 (1997) 362–365.
[24] D.D. Lasic, Novel applications of liposomes, Trends Biotech. 16 (1998) 307–321.
[25] T. Lian, R.J. Ho, Trends and developments in liposome drug delivery systems, J. Pharm. Sci. 90 (2001) 667–680.
[26] T.M. Allen, P.R. Cullis, Drug delivery systems: entering the mainstream, Science 303 (2004) 1818–1822.
[27] V.P. Torchilin, Recent advances with liposomes as pharmaceutical carriers, Nat. Rev. Drug Discov. 4 (2005) 145–160.
[28] I.W. Kellaway, S.J. Farr, Liposomes as drug delivery systems to the lung, Adv. Drug Deliv. Rev. 5 (1990) 149–161.
[29] D. Papahadjopoulos, T.M. Allen, A. Gabizon, E. Mayhew, K. Matthay, S.K. Huang, K.D. Lee, M.C. Woodle, D.D. Lasic, C. Redemann, Sterically stabilized liposomes: improvements in pharmacokinetics and antitumor therapeutic efficacy, Proc. Natl. Acad. Sci. USA 88 (1991) 11460–11464.
[30] T.M. Allen, C. Hansen, Pharmacokinetics of stealth versus conventional liposomes: effect of dose, Biochim. Biophys. Acta 1068 (1991) 133–141.
[31] M.C.Woodle, Woodle, D.D.Lasic, Lasic, Sterically stabilized liposomes, Biochim. Biophys. Acta 1113 (1992) 171–199.
[32] M. Huang, O.P. Rorstad, VIP receptors in mesenteric and coronary arteries: a radioligand binding study, Peptides 8 (1987) 477–485.
[33] I. Rubinstein, M. Patel, H. Ikezaki, S. Dagar, H. Onyuksel, Conformation and vasoreactivity of VIP in phospholipids: effects of calmodulin, Peptides 20 (1999) 1497–1501.
[34] H. Suzuki, Y. Noda, S. Paul, X.P. Gao, I. Rubinstein, Encapsulation of vasoactive intestinal peptide into liposomes: effects on vasodilation in vivo, Life Sci. 57 (1995) 1451–1457.
[35] J.C. Waldrep, New aerosol drug delivery systems for the treatment of immune-mediated pulmonary diseases, Drugs Today (Barc.) 34 (1998) 549–561.
[36] S.A. Cryan, Carrier-based strategies for targeting protein and peptide drugs to the lungs, AAPS J. 7 (2005) 20–41.
[37] R. Niven, Modulated drug therapy with inhalation aerosols, in: A.J. Hickey (Ed.), Pharmaceutical Inhalation Aerosols Technology, Marcel Dekker, New York, 2003, pp. 551–570.
[38] S. Anabousi, E. Kleemann, U. Bakowsky, T. Kissel, T. Schmehl, T. Gessler, W. Seeger, C.M. Lehr, C. Ehrhardt, Effect of PEGylation on the stability of liposomes during nebulisation and in lung surfactant, J. Nanosci. Nanotechnol. 6 (2006) 3010–3016.
[39] R. Wattiez, P. Falmagne, Proteomics of bronchoalveolar lavage fluid, J. Chromatogr. B Analyt. Technol. Biomed. Life Sci. 815 (2005) 169–178.
[40] C. Vermehren, S. Frokjaer, T. Aurstad, J. Hansen, Lung surfactant as a drug delivery system, Int. J. Pharm. 307 (2006) 89–92.
[41] J. Wu, M. Kobayashi, E.A. Sousa, W. Liu, J. Cai, S.J. Goldman, A.J. Dorner, S.J. Projan, M.S. Kavuru, Y. Qiu, M.J. Thomassen, Differential proteomic analysis of bronchoalveolar lavage fluid in asthmatics following segmental antigen challenge, Mol. Cell. Proteomics 4 (2005) 1251–1264.
[42] A. Plymoth, C.G. Lofdahl, A. Ekberg-Jansson, M. Dahlback, H. Lindberg, T.E. Fehniger, G. Marko-Varga, Human bronchoalveolar lavage: biofluid analysis with special emphasis on sample preparation, Proteomics 3 (2003) 962–972.
[43] R.H. Notter, Lung surfactant, in: Basic Science and Clinical Applications, Marcel Dekker, Inc., New York, 2000, pp. 1–444.
[44] B.A. Hills, Surface-active phospholipid: a Pandora's box of clinical applications. Part I. The lung and air spaces, Intern. Med. J. 32 (2002) 170–178.
[45] I. Noel-Georis, A. Bernard, P. Falmagne, R. Wattiez, Database of bronchoalveolar lavage fluid proteins, J. Chromatogr. B Analyt. Technol. Biomed. Life Sci. 771 (2002) 221–236.
[46] B. Stark, P. Debbage, F. Andreae, W. Mosgoeller, R. Prassl, Association of vasoactive intestinal peptide with polymer-grafted liposomes: structural aspects for pulmonary delivery, Biochim. Biophys. Acta 1768 (2007) 705–714.
[47] G.R. Bartlett, Phosphorus assay in column chromatography, J. Biol. Chem. 234 (1959) 466–468.
[48] Y. Chen, J.D. Muller, K.M. Berland, E. Gratton, Fluorescence fluctuation spectroscopy, Methods 19 (1999) 234–252.
[49] Y. Chen, J.D. Muller, P.T. So, E. Gratton, The photon counting histogram in fluorescence fluctuation spectroscopy, Biophys. J. 77 (1999) 553–567.
[50] M. Edetsberger, E. Gaubitzer, E. Valic, E. Waigmann, G. Kohler, Detection of nanometer-sized particles in living cells using modern fluorescence fluctuation methods, Biochem. Biophys. Res. Commun. 332 (2005) 109–116.
[51] S.T. Hess, S. Huang, A.A. Heikal, W.W. Webb, Biological and chemical applications of fluorescence correlation spectroscopy: a review, Biochemistry 41 (2002) 697–705.
[52] P. Kask, K. Palo, D. Ullmann, K. Gall, Fluorescence-intensity distribution analysis and its application in biomolecular detection technology, Proc. Natl. Acad. Sci. USA 96 (1999) 13756–13761.
[53] J.D. Muller, Y. Chen, Q.Q. Ruan, W.W. Mantulin, E. Gratton, Resolving heterogeneuos sample populations with the photon counting histogram method, Biophys. J. 76 (1 Pt 2) (1999) A359.
[54] P. Schwille, U. Haupts, S. Maiti, W.W. Webb, Molecular dynamics in living cells observed by fluorescence correlation spectroscopy with one- and two-photon excitation, Biophys. J. 77 (1999) 2251–2265.
[55] P. Kask, K. Palo, U. Mets, M. Cole, M.K. Gall, Fluorescence intensity distribution analysis (FIDA) and related fluorescence fluctuation techniques: theory and practice, in: R. Krayenhof, A.J.W.G. Visser, H.C. Gerrritsen (Eds.), Fluorescence Spectroscopy, Imaging and Probes, Springer, 2002, pp. 154–171.
[56] R.M. Robinson, E.W. Blakeney Jr., W.L. Mattice, Lipid-induced conformational changes in glucagon, secretin, and vasoactive intestinal peptide, Biopolymers 21 (1982) 1228–1271.
[57] J.M. Harris, N.E. Martin, M. Modi, Pegylation: a novel process for modifying pharmacokinetics, Clin. Pharmacokinet. 40 (2001) 539–551.
[58] M.L. Nucci, R. Shorr, A. Abuchowski, The therapeutic value of poly(ethylene glycol)-modified proteins, Adv. Drug. Deliv. Rev. 6 (1991) 133–151.
[59] C. Delgado, G.E. Francis, D. Fisher, The uses and properties of PEG-linked proteins, Crit. Rev. Ther. Drug Carrier Syst. 9 (1992) 249–304.
[60] P. Stiuso, A. Marabotti, A. Facchiano, M. Lepretti, A. Dicitore, P. Ferranti, M. Carteni, Assessment of the conformational features of vasoactive intestinal peptide in solution by limited proteolysis experiments, Biopolymers 81 (2006) 110–119.